



# CT analysis of the posterior anatomical landmarks of the scoliotic spine



I.N. Tromp<sup>a</sup>, R.C. Brink<sup>a</sup>, J.F. Homans<sup>a</sup>, T.P.C. Schlösser<sup>a</sup>, M. van Stralen<sup>b</sup>,  
M.C. Kruyt<sup>a,\*</sup>, W.C.W. Chu<sup>c</sup>, J.C.Y. Cheng<sup>d</sup>, R.M. Castelein<sup>a</sup>

<sup>a</sup> Department of Orthopaedic Surgery, University Medical Centre Utrecht, Utrecht, the Netherlands

<sup>b</sup> Imaging Division, University Medical Centre Utrecht, Utrecht, the Netherlands

<sup>c</sup> Department of Imaging and Interventional Radiology, Prince of Wales Hospital, The Chinese University of Hong Kong, Shatin, Hong Kong, China

<sup>d</sup> Department of Orthopaedics and Traumatology, Prince of Wales Hospital, The Chinese University of Hong Kong, Shatin, Hong Kong, China

## ARTICLE INFORMATION

### Article history:

Received 17 November 2021

Received in revised form

24 July 2022

Accepted 25 July 2022

**AIM:** To use computed tomography (CT) to assess the validity and reliability of the posterior landmarks, spinous processes (SP), transverse processes (TP), and centre of lamina (COL), as compared to the Cobb angle to assess the curve severity and progression of adolescent idiopathic scoliosis (AIS).

**MATERIALS AND METHODS:** A consecutive series of CT examinations of severe AIS patients were included retrospectively. SP, TP, and COL angles were measured for all curves and compared to the Cobb angle.

**RESULTS:** One hundred and five patients were included. The mean Cobb versus SP, TP, and COL angles were, 54° versus 37°, 49°, and 51° in the thoracic curves and 34° versus 26°, 31°, and 34° in the (thoraco)lumbar curves. Intraclass correlation coefficient values for intra-rater measurements of the SP, TP, and COL angles were 0.93, 0.97, and 0.95 and 0.70, 0.90, and 0.88 for inter-rater measurements. The correlations between the Cobb angle and SP, TP, and COL angles in thoracic and (thoraco)lumbar curves were 0.79 and 0.66, 0.87 and 0.84, and 0.80 and 0.70.

**CONCLUSIONS:** The posterior spinal landmarks can be used for assessment of scoliosis severity in AIS; however, they show a systematic underestimation, but a strong correlation with the coronal Cobb angle. TP and COL angles had the highest validity.

© 2022 The Authors. Published by Elsevier Ltd on behalf of The Royal College of Radiologists. This is an open access article under the CC BY license (<http://creativecommons.org/licenses/by/4.0/>).

\* Guarantor and correspondent: M. C. Kruyt, Department of Orthopaedic Surgery, G05.228, University Medical Centre Utrecht, P.O. Box 85500, 3508 GA Utrecht, the Netherlands. Tel.: +31887554578; fax: +31302510638.

E-mail address: [M.C.Kruyt@umcutrecht.nl](mailto:M.C.Kruyt@umcutrecht.nl) (W.C. Kruyt).

## Introduction

The coronal Cobb angle, as measured on upright posterior–anterior radiographs, is the reference standard to assess curve severity and progression of adolescent idiopathic scoliosis (AIS).<sup>1,2</sup> AIS patients often undergo repeated radiographs to document progression of the deformity or treatment effectiveness, and this covers a relatively long period during their adolescence, at the time that gonadal and breast tissue mature. Simony *et al.* described a five-times higher overall cancer rate in a Danish AIS population, as compared to age-matched controls.<sup>3</sup>

Several radiation-free imaging methods are available to measure the severity of the scoliosis, such as surface topography and ultrasound imaging.<sup>4–14</sup> In this, surface topography has been studied for decades, but the asymmetry of the torso is influenced by spine shape, as well as the ribcage, trunk rotation, muscle volume, body fat, and posture. Three-dimensional (3D) ultrasound imaging of the spine as a radiation-free alternative method of measuring spinal curvature, has gained growing attention and its feasibility has been demonstrated in several recent studies.<sup>4–6,8–11,13–20</sup> These studies showed that the spinous processes (SP), transverse processes (TP), and centre of lamina (COL) can be used as anatomical landmarks to assess spinal curve severity. It is important to note that ultrasound only visualises the posterior elements of the spine, not the vertebral endplates, and thus gives a different projection of the 3D deformity than the conventional coronal Cobb angle measured on radiographs or computed tomography (CT). Brink *et al.* showed a small difference in rotation of the posterior elements as compared to the vertebral bodies on CT.<sup>21</sup> The exact relationship between the conventional coronal Cobb angle, which is based on the orientation of the anteriorly located vertebral bodies, and the orientation of the posterior landmarks for the assessment of severity of the scoliotic spine remains unknown.

The aim of this study was to investigate the relationship between the different anatomical landmarks (SP, TP, COL, and vertebral endplates) on CT and to test the reliability and validity of these landmarks for curve severity measurements.

## Materials and methods

### Population

Institutional review board approval was provided by the Joint CUHK-NTEC CREC (reference no. 2013.386) and all patients enrolled in this study provided written informed consent. From an existing database of a consecutive series of 108 AIS patients with preoperative high-resolution CT images (0.625 mm section thickness, 64-section multi-detector scanner; GE Healthcare, Chalfont, St Giles, UK) scheduled for scoliosis surgery in one academic centre between 2010 and 2016<sup>22</sup> were included. CT examinations were obtained in the prone position as part of the preoperative work-up for navigation purposes. No new imaging was undertaken for the purposes of this study. Inclusion criteria were diagnosis

of AIS and scheduled for AIS surgery between 2010 and 2016. Exclusion criteria were incomplete CT, other spinal pathology, previous spinal surgery, neurological symptoms, or neural axis abnormalities on preoperative magnetic resonance imaging (MRI), or atypical left convex thoracic curves or right convex (thoraco)lumbar curves.

### CT measurements

Using a previously validated method for semi-automatic analysis (ScoliosisAnalysis 1.3 Imaging Division, Utrecht, The Netherlands), complete 3D spinal reconstruction were acquired. The conventional coronal Cobb angle was determined by manual measurement of the angle between the two most tilted cranial and caudal vertebral endplates in the curve on a reconstructed coronal projection.<sup>1</sup> Thereafter, the exact location of the tip of both the postero-caudal SP and supero-lateral TP as well as the deepest point of the COL were identified manually in the 3D reconstruction and extracted into a Cartesian 3D coordinate system (Fig 1). The SP angle

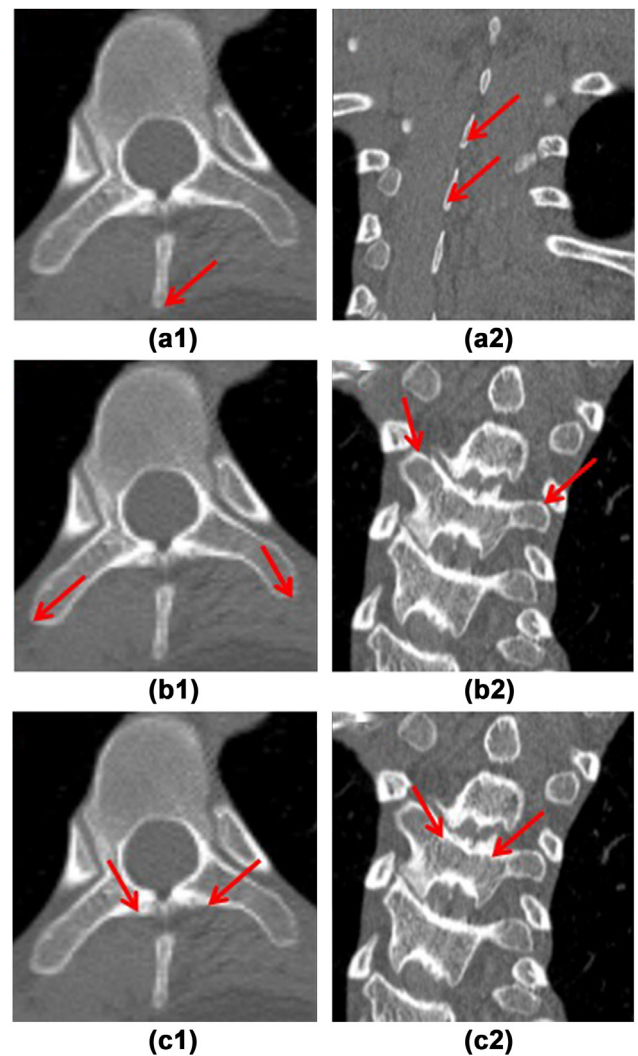


**Figure 1** CT image of (1) transversal and (2) coronal view of a vertebra with marked in red the location of the (a) SP tip (b) TP tip, and (c) COL point used for CT measurements.

was determined as the angle between the most tilted line connecting two consecutive SPs at the cranial and caudal end of the curves ([Electronic Supplementary Material Fig. S1](#)). The TP angle was determined as the angle between the most tilted line connecting the left and right tip of the TP at the cranial curve and the most tilted line connecting the left and right side of one TP at the caudal curve ([Electronic Supplementary Material Fig. S1](#)) and the COL angle was determined as the angle between the most tilted line connecting the left and right centre of lamina at the cranial curve and the most tilted line connecting the left and right lamina at the caudal curve ([Electronic Supplementary Material Fig. S1](#)).

### Statistical analysis

Statistical analyses were performed using SPSS Statistics 25 for Windows (SPSS, Chicago, IL, USA). For descriptive statistics, mean, standard deviation, and ranges were provided. Normality of data was assessed using graphical methods (Q-Q plots and histograms). The mean absolute error (MAE) was used to describe the difference between the Cobb angle and the anatomical landmark angles and the paired *t*-tests to test these differences. For intra- and inter-observer reliability, two observers trained as orthopedic residents (I.N.T. twice, R.C.B. once) analysed a random subset of 16 CT examinations of AIS patients on separate sittings. The intra- and inter-rater reliability was calculated as (two-way random effects model and absolute agreement) intraclass correlation coefficient (ICC). The correlation between the Cobb angle and the anatomical landmarks angles were determined using Pearson's correlation (*r*). The agreement of the anatomical landmark angle measurements and the Cobb angle was tested by using the Bland–Altman method. Using the Bland–Altman plot the agreement between the ultrasound and Cobb angle and possible outliers was described. For all analyses, the significance level was set at 0.05.

## Results

At total of 105 patients were included out of the database with 108 presurgical scoliosis patients (three excluded because CT was inadequate). Mean age was  $16.3 \pm 2.7$  (range 10–26.4) years, 84% of the patients were female ([Table 1](#)).

### Validity

The mean ( $\pm$ standard deviation) of the conventional Cobb angle versus SP angle, TP angle and COL angle of the thoracic curves were:  $54^\circ \pm 14^\circ$ (Cobb),  $37^\circ \pm 11^\circ$  (SP),

**Table 1**  
Demographics of the included adolescent idiopathic scoliosis (AIS) patients.

		AIS patients (n=105)
Age in years	Mean $\pm$ SD	16.3 $\pm$ 2.7
	Range	10.0–26.4
Female	n (%)	89 (84)

$49^\circ \pm 13^\circ$  (TP) and  $51^\circ \pm 13^\circ$  (COL). For the (thoraco)lumbar curves the angles were  $34^\circ \pm 14^\circ$  (Cobb),  $26^\circ \pm 9^\circ$  (SP),  $31^\circ \pm 12^\circ$  (TP) and  $34^\circ \pm 14^\circ$  (COL), respectively ([Table 2](#)). The MAE between the Cobb angle and the anatomical landmark angles were;  $14^\circ$  (Cobb–SP),  $7^\circ$  (Cobb–TP) and  $7^\circ$  (Cobb–COL;  $p \leq 0.01$ ). Linear regression showed that the correlations between SP and conventional Cobb angle were 0.79 for main thoracic curves and 0.66 for (thoraco)lumbar curves. The correlations between the TP and conventional Cobb angle were 0.87 (thoracic) and 0.84 ((thoraco)lumbar) and 0.80 and 0.70 between the COL and conventional Cobb angle ( $p \leq 0.01$ ; [Fig 2](#)). The Bland–Altman plot showed a difference between the anatomical landmark angles and the Cobb angle measurements ([Fig 3](#)).

### Reliability

Intra-rater reliability analyses showed the following values: SP angle ICC = 0.93, TP angle ICC = 0.97, and COL angle ICC = 0.95, whereas the inter-rater reliability values were ICC = 0.70 (SP angle), ICC = 0.90 (TP angle), and ICC = 0.88 (COL angle; [Table 3](#)).

## Discussion

Scoliosis severity is traditionally assessed on a standing coronal radiograph employing the Cobb angle measurement, the angle that is formed by the two most tilted vertebral bodies in the curve.<sup>1</sup> All newer imaging methods should be validated against this reference standard. 3D ultrasound imaging of the spinal curvature has gained growing attention as a rising radiation-free alternative method to evaluate the morphology of the spine.<sup>4,6,9,11,14–20</sup> 3D spinal ultrasound, however, can only visualise the posterior elements of the spine and therefore gives a different projection of the rotated vertebrae than the traditional Cobb angle measurement, which is based on the projection of the anteriorly located vertebral bodies. To date, different anatomical landmarks have been described as an ultrasound alternative for the Cobb angle, such as the SP, TP, and the COL.<sup>4,6,9,11,14–20</sup> The exact relation between the posterior structures accessible by ultrasound (SP, TP, COL) and the vertebral endplates, as normally used on radiographs, remains unclear. Although several 3D (reconstructed)

**Table 2**  
Cobb, spinous processes (SP), transverse processes (TP) and centre of lamina (COL) angle characteristics measured on computed tomography.

	Mean $\pm$ SD ( $^\circ$ )
Thoracic curves	
Cobb angle	54 $\pm$ 14
SP angle	37 $\pm$ 11
TP angle	49 $\pm$ 13
COL angle	51 $\pm$ 13
(Thoraco)lumbar curves	
Cobb angle	34 $\pm$ 14
SP angle	26 $\pm$ 9
TP angle	31 $\pm$ 12
COL angle	34 $\pm$ 14

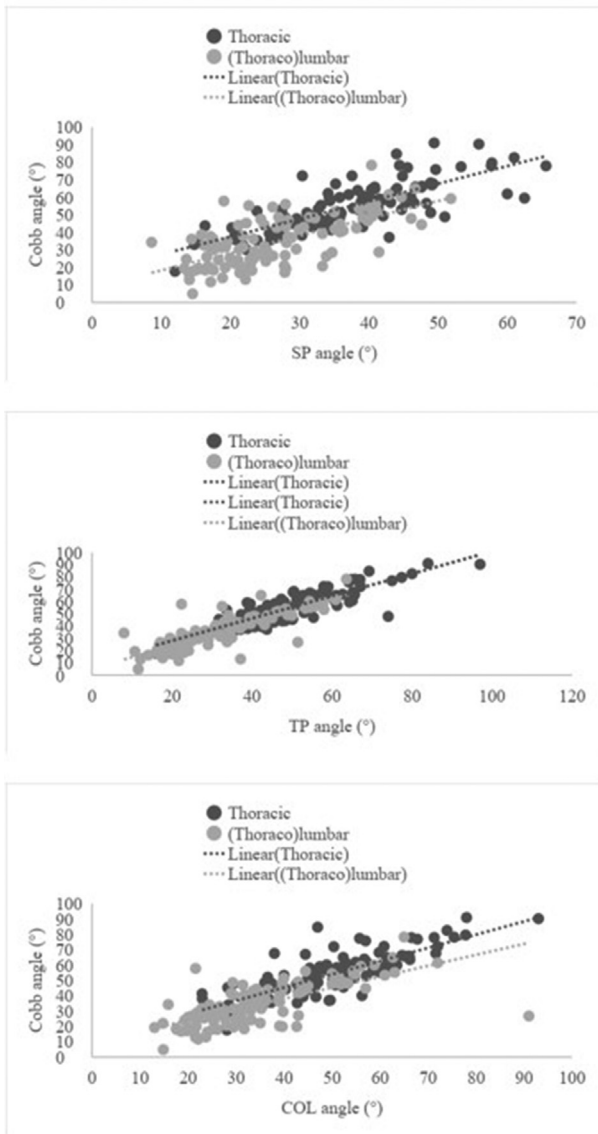


**Figure 2** Pearson's correlations ( $r$ ) and the equations between the Cobb angle on the y-axis and the anatomical landmark angles on the x-axis. The SP angle, TP angle, and COL angle are shown for the thoracic (black) and (thoraco)lumbar (grey) curves.

imaging methods are available, such as MRI and low-dose biplanar radiography (EOS system), CT is still considered as the reference standard for providing accurate and detailed information on bony anatomy and can give accurate 3D reconstructions of complex deformities in each desired plane.<sup>23</sup> In this study, an existing database of CT imaging is used to provide important and exact information about the relations between the different anterior and posterior anatomical landmarks for assessment of curve severity.

The anatomical landmarks, as based on these CT analyses, showed different angles than the coronal Cobb method. The difference in curve severity measurements between the SP, TP, COL, and the Cobb angle can be explained by the different spinal structures used for the

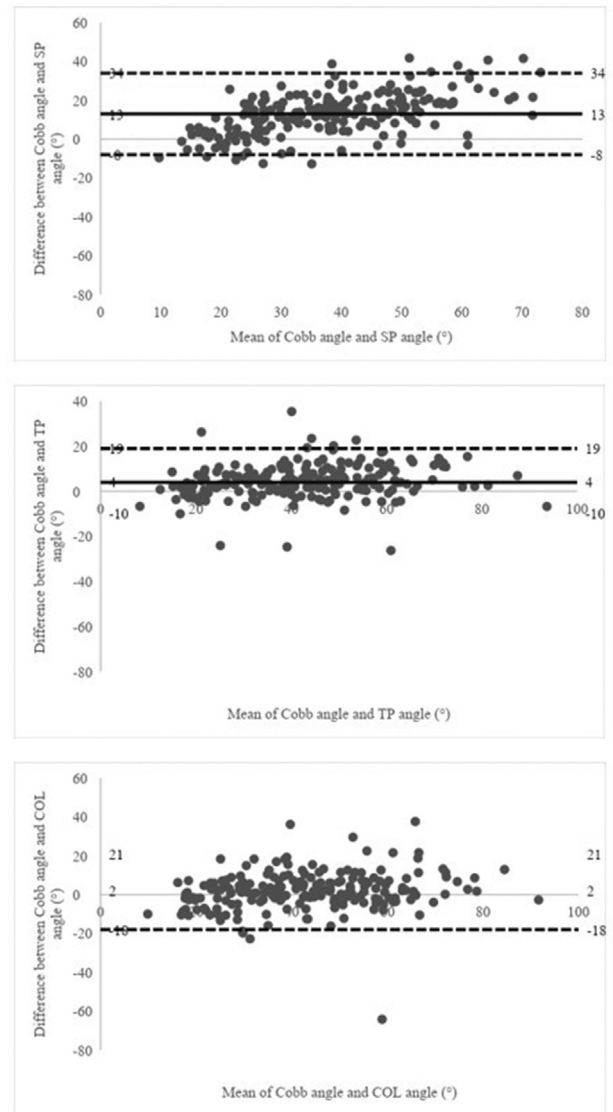


**Figure 3** Bland–Altman plots that show the agreement between the Cobb angles and the SP, TP, and COL angles.

angle measurements and their position in space. Although the TP and COL method are similar to the Cobb method, as the endplates of the vertebral body are along the same line as the TP and COL lines used, the SP line is along a different direction from the Cobb method. It is well known that in scoliosis, the posterior structures, such as the spinous processes, describe less of an arc than the vertebral bodies that are rotated and tilted farther from the midline.<sup>24</sup>

**Table 3**

Reliability of the anatomical landmarks angles with the Cobb angle on computed tomography measured with intraclass correlation coefficient.

	Intra-rater reliability	Inter-rater reliability
Spinous processes angle	0.93	0.70
Transverse processes angle	0.97	0.90
Centre of lamina angle	0.95	0.88

In this CT based study, moderate to excellent correlations were found between the angles measured using the posterior anatomical landmarks versus the conventional Cobb angle (thoracic  $r \geq 0.79$  and (thoraco)lumbar  $r \geq 0.66$ ). The present findings could not be correlated to ultrasound measurements because no ultrasound measurements were made of the spinal curve of the patients that were included in this study, as this was not the purpose of the study. In a clinical study, Brink *et al.* showed excellent linear correlations between SP and TP ultrasound angles and the radiographic Cobb angle (thoracic  $R^2 \geq 0.987$  and (thoraco)lumbar  $R^2 \geq 0.970$ ).<sup>15</sup> Because of the use of high-resolution CT imaging, there are practical differences between the present findings and those of Brink *et al.* In this study, the exact tip of the SP and TP was used for the angle measurements, while with the ultrasound method, it is not completely clear whether the exact tip of the SP and TP, or part of the bases of the processes, which are more closely related to the vertebral bodies, are used for the measurements. This accuracy might have led to different correlations in comparison to the validation study for ultrasound-based Cobb angle measurements. In addition, Wang *et al.* showed a high correlation between the COL angle on ultrasound and the coronal Cobb angle on MRI ( $r > 0.9$ ).<sup>11</sup> An explanation for the slight differences with the present findings could be the fact that only 16 patients were included and the average Cobb angle was  $21.7 \pm 15.9^\circ$ , while the present study included far more patients, curves were bigger, and a distinction was made between thoracic and (thoraco)lumbar curves. CT scans from an existing database of preoperative AIS patients were used; no new imaging was undertaken for the purposes of this study.

Limitations of the current study are the prone position of the patients for CT, which differs from the upright position for traditional radiological curve assessment; however, all the measurements (landmarks and Cobb angles) are based on the same CT images and involve osseous elements of which the relation will not be influenced by the positioning of the patients.<sup>25,26</sup> Another limitation is that only moderate to severe AIS curves were included. As a consequence, the exact relation between the landmarks and actual Cobb angle may be different in less pronounced curves. Nevertheless, the feasibility to use these landmarks and the consistency of the relation was demonstrated. Angles, based on the SP, TP, and COL are representative of the more anteriorly located endplates and therefore represent curve severity. When comparing the reliability of the anatomical landmark angles to the Cobb angle the TP angle has the highest intra- and inter-rater correlations. This can be explained by the fact that the TP measurement method is more similar to the measurement of the Cobb angle by using tilted lines instead of only one point per vertebra, as with the SP measurement.

In this study, CT images were used to assess the relationship between the Cobb angle (based on the vertebral bodies) and several angles based on the posterior structures. As expected, the posterior-element-based SP, TP, and COL angles represent different values in comparison to the endplate-based Cobb angle. As these anatomical landmarks

are located more posteriorly and project differently in the coronal plane than the vertebral bodies, on average, they systematically underestimate the curve angle as compared to the conventional Cobb angle. The SP, TP, and COL are valid and reliable anatomical landmarks for coronal curve assessment, from which the TP and COL angles correlate best with the traditional Cobb angle.

## Conflict of interest

The authors declare the following financial interests/personal relationships which may be considered as potential competing interests: R.M. Castelein reports financial support was provided by unrestricted K2M research grant. I.N. Tromp reports a relationship with Cotrel Foundation that includes: funding grants. I.N. Tromp reports a relationship with Eurospine TFR grant that includes: funding grants. R.M. Castelein reports a relationship with Cotrel Foundation that includes: funding grants. R.M. Castelein reports a relationship with Eurospine TFR grant that includes: funding grants. R.M. Castelein reports a relationship with unrestricted K2M research grant that includes: funding grants.

## Acknowledgements

This work was financially supported by an unrestricted K2M research grant. I.N.T. reports grants from Cotrel Foundation, grants from Eurospine TFR, outside the submitted work. R.M.C. reports grants from unrestricted K2M research grant, grants from Cotrel Foundation, grants from Eurospine TFR, outside the submitted work.

## Appendix A. Supplementary data

Supplementary data to this article can be found online at <https://doi.org/10.1016/j.crad.2022.07.013>.

## References

1. Cobb JR. Outline for the study of scoliosis. In: Edwards JW, editor. *AAOS, Instructional Course Lectures* vol. 5. Ann Arbor, MI: The American Academy of Orthopaedic Surgeons; 1948. p. 261–75.
2. Cheng JC, Castelein RM, Chu WC, *et al.* Adolescent idiopathic scoliosis. *Nat Rev Dis Prim* 2015;1:15030.
3. Simony A, Hansen EJ, Christensen SB, *et al.* Incidence of cancer in adolescent idiopathic scoliosis patients treated 25 years previously. *Eur Spine J* 2016;25:3366–70.
4. Li M, Cheng J, Ying M, *et al.* Could clinical ultrasound improve the fitting of spinal orthosis for the patients with AIS? *Eur Spine J* 2012;21:1926–35.
5. Chen W, Le LH, Lou EHM. Ultrasound imaging of spinal vertebrae to study scoliosis. *Open J Acoust* 2012;2:95–103.
6. Chen W, Lou EHM, Zhang PQ, *et al.* Reliability of assessing the coronal curvature of children with scoliosis by using ultrasound images. *J Child Orthop* 2013;7:521–9.
7. Komeili A, Westover L, Parent EC, *et al.* Correlation between a novel surface topography asymmetry analysis and radiographic data in scoliosis. *Spine Deform* 2015;3:303–11.
8. Vo QN, Lou EHM, Le LH. Measurement of axial vertebral rotation using three-dimensional ultrasound images. *Scoliosis* 2015;10:S7.

9. Young M, Hill DL, Zheng R, et al. Reliability and accuracy of ultrasound measurements with and without the aid of previous radiographs in adolescent idiopathic scoliosis (AIS). *Eur Spine J* 2015;**24**:1427–33.
10. Nguyen DV, Vo QN, Le LH, et al. Validation of 3D surface reconstruction of vertebrae and spinal column using 3D ultrasound data—a pilot study. *Med Eng Phys* 2015;**37**:239–44.
11. Wang Q, Li M, Lou EHM, et al. Reliability and validity study of clinical ultrasound imaging on lateral curvature of adolescent idiopathic scoliosis. *PLoS One* 2015;**10**:e0135264.
12. Knott P, Sturm P, Lonner B, et al. Multicentre comparison of 3D spinal measurements using surface topography with those from conventional radiography. *Spine Deform* 2016;**4**:98–103.
13. Zheng R, Young M, Hill D, et al. Improvement on the accuracy and reliability of ultrasound coronal curvature measurement on adolescent idiopathic scoliosis with the aid of previous radiographs. *Spine (Phila Pa 1976)* 2016;**41**:404–11.
14. Zheng Y-P, Lee TT-YT, Lai KK-LK, et al. A reliability and validity study for Scolioscan: a radiation-free scoliosis assessment system using 3D ultrasound imaging. *Scoliosis Spinal Disord* 2016;**11**:1–15.
15. Brink RC, Wijdicks SPJ, Tromp IN, et al. A reliability and validity study for different coronal angles using ultrasound imaging in adolescent idiopathic scoliosis. *Spine J* 2017;**18**:979–85.
16. Lou EH, Chan ACY, Donauer A, et al. Ultrasound-assisted brace casting for adolescent idiopathic scoliosis, IRSSD Best research paper 2014. *Scoliosis* 2015;**10**:8–13.
17. Li M, Cheng J, Ying M, et al. A preliminary study of estimation of Cobb's angle from the spinous process angle using a clinical ultrasound method. *Spine Deform* 2015;**3**:476–82.
18. Zheng R, Chan ACY, Chen W, et al. Intra- and inter-rater reliability of coronal curvature measurement for adolescent idiopathic scoliosis using ultrasonic imaging method—a pilot study. *Spine Deform* 2015;**3**:151–8.
19. Cheung CWJ, Zhou GQ, Law SY, et al. Ultrasound volume projection imaging for assessment of scoliosis. *IEEE Trans Med Imaging* 2015;**34**:1760–8.
20. Ungi T, King F, Kempston M, et al. Spinal curvature measurement by tracked ultrasound snapshots. *Ultrasound Med Biol* 2014;**40**:447–54.
21. Brink RC, Schlösser TPC, Colo D, et al. Asymmetry of the vertebral body and pedicles in the true transverse plane in adolescent idiopathic scoliosis: a CT-based study. *Spine Deform* 2017;**5**:37–45.
22. Chen H, Schlösser TPC, Brink RC, et al. The height–width–depth ratios of the intervertebral discs and vertebral bodies in adolescent idiopathic scoliosis vs controls in a Chinese population. *Sci Rep* 2017;**7**:46448.
23. Glaser DA, Doan J, Newton PO. Comparison of 3-dimensional spinal reconstruction accuracy: biplanar radiographs with EOS versus computed tomography. *Spine (Phila Pa 1976)* 2012;**37**:1391–7.
24. Herzenberg JE, Waanders NA, Closkey RF, et al. Cobb angle versus spinous process angle in adolescent idiopathic scoliosis: the relationship of the anterior and posterior deformities. *Spine (Phila Pa 1976)* 1990;**15**:874–9.
25. Brink RC, Colo D, Schlösser TPC, et al. Upright, prone, and supine spinal morphology and alignment in adolescent idiopathic scoliosis. *Scoliosis Spinal Disord* 2017;**12**:6.
26. Brink RC, Schlösser TPC, van Stralen M, et al. Anterior–posterior length discrepancy of the spinal column in adolescent idiopathic scoliosis—a 3D CT study. *Spine J* 2018;**18**:2259–65.
27. Brink RC. *Consequences of the Three-Dimensional Pathoanatomy of Adolescent Idiopathic Scoliosis*. Unpublished doctoral dissertation. Utrecht University; 2019.

## Further reading